Journal of Materials Chemistry C

Accepted Manuscript

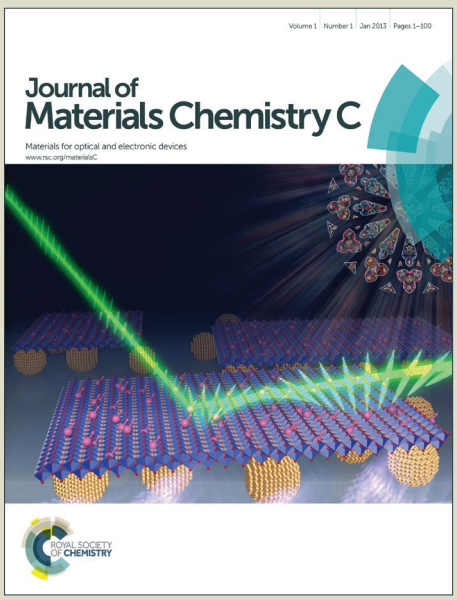

ROYAL SOCIETY OF CHEMISTRY

www.rsc.org/materialsC

Jounal of Materials Chemistry C

COMMUNICATION

$NaYF_4:Yb^{3+},Tm^{3+}$ Inverse Opal Photonic Crystals and $NaYF_4:Yb^{3+},Tm^{3+}/TiO_2$ composites: Synthesis, Highly Improved Upconversion Properties and NIR Photoelectric Response

Received 00th January 20xx,
Accepted 00th January 20xx

DOI: 10.1039/x0xx00000x

www.rsc.org/

Yudan Yang,[ba] Pingwei Zhou,[a] Wen Xu,[a] Sai Xu,[a] Yandong Jiang,[a] Xu Chen[a] and Hongwei Song*[a]

A novel solvent-thermal Y_2O_3 template method was explored to synthesis $NaYF_4:Yb^{3+},Tm^{3+}$ inverse opal photonic crystals (IOPCs), which shows highly improved up-conversion luminescence properties.

Up-conversion luminescence (UCL) which convert two or more near infrared (NIR) photons to one visible or UV photon could be useful for various technological applications such as solar cells, short wavelength solid state lasers, optical data storage, infrared photocatalysis, infrared-responsive devices, biological fluorescence labels and white light emitters, etc.[1] Among various UC materials, inorganic compounds doped with trivalent rare-earth (RE) ions have emerged as the most promising media duo to the ladder-like 4f energy levels, which shows superior in many aspects such as multiple emissions, controllable and narrow emission band, higher conversion efficiency, better photostability and chemical durability.[2] Fluoride has been demonstrated to be promising host materials for UCL because of its low phonon energy. However, the lower UCL efficiency is still a bottleneck problem for various applications. At present, various methods have been explored to improve the UC strengths.[3] Exploring of more strategies to enhance UCL processes would be profound significance.

On the other hand, since the concept of photonic crystals (PhCs) was first mentioned by Yablonovitch[4] and John[5] in 1987, these special structures have attracted considerable attentions in the fields of near-zero threshold lasers, sensors, waveguides, PhC fibers and etc.[6] In recent years, the modulations of IOPC structures on UCL properties of RE-ions were also widely studied.[7] However, only a few prepared fluoride($NaYF_4$) based IOPC composites by the direct template method due to preparation difficulties.[8] It is necessary to develop novel methods to prepare fluoride IOPCs and fully understand the effects of PhC structure on the UCL processes RE-ions in the fluorides with lower phonon energy.

In this work, $NaYF_4$ IOPCs were successfully prepared through a novel solvent-thermal Y_2O_3 IOPC template method and the phase of $NaYF_4:Tm^{3+}/Er^{3+}$ and the photonic band gap（PBG）of IOPCs could be adjusted by pH value, reaction time and template. Subsequently, the UCL properties and dynamics were systematically studied and the results show that the IOPC structure is conductive to UCL, especially for high-order UC processes. And more, the NIR photoelectric response was observed in $NaYF_4$: Yb, Tm IOPCs/TiO_2 system, indicating this special material has a good application prospect in the field of photocatalyses and photoelectrochemistry.

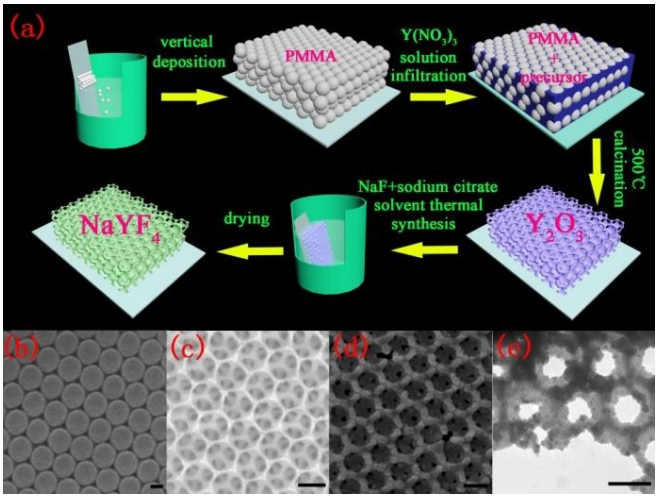

Fig. 1(a) Schematic of the fabrication processes using a solvent-thermal method for $NaYF_4$ IOPCs. The SEM image of PMMA opal template (b), Y_2O_3 inverse opal template (c), $NaYF_4$ IOPC (d) and the TEM image of NaYF4 IOPC (e).The scale bar is 200 nm.

Fig. 1(a) shows the schematic of fabrication processes of $NaYF_4$ IOPCs, and the detail description is shown in the supporting information. The SEM images of PMMA opal template, Y_2O_3 IOPC template and $NaYF_4$ IOPC were shown in Fig. 1(b)-1(d), which demonstrated a high degree of ordered PhC structure of face-centered-cubic (FCC) arrays. Note that the center-to-center distance of $NaYF_4$ IOPC is the same as the Y_2O_3 IOPC template, indicating that the solvent-thermal process is occurred around the IOPC skeleton

[a] State Key Laboratory on Integrated Optoelectronics, College of Electronic Science and Engineering, Jilin University, Changchun, 130012, People's Republic of China;Fax:86-431-85155129;Tel:86-431-85155129; Email:songhw@jlu.edu.cn.
[b] China-Japan Union Hospital, Jilin University, Changchun, 130033, People's Republic of China;Fax:86-431-84995382;Tel:86-431-849953802;E-mail: yangyudan@jlu.edu.cn.

† Electronic Supplementary Information (ESI) available: Experimental section and Fig. S1–S3. See DOI: 10.1039/x0xx00000x

and did not destroy the IOPC structure. Figure 1(e) shows the TEM image of the $NaYF_4$ IOPC, which shows an ordered empty cavity structure consisting of $NaYF_4$ walls and further indicates the well-ordered IOPC structure.

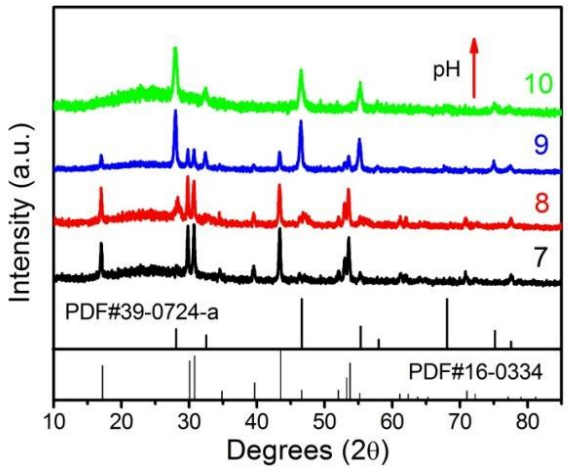

Fig. 2 The XRD patterns of $NaYF_4$ IOPCs with different pH values.

In solvent-thermal process, pH value is an important parameter which directly affects the phase and structure of $NaYF_4$ IOPCs. The temperature and the reaction time are controlled to be 180 °C and 2 h, and the pH value is adjusted to be 1, 4, 7, 8, 9 and 10 with nitric acid or ammonia, respectively. When the pH value is less than 7, the Y_2O_3 IOPC skeleton is completely dissolved away under the action of large amount of H^+; When the pH value is equal to or larger than 7, the IOPC structure could be better inherited. As shown in Fig. 2, in the neutral condition, the hexagonal is dominant. With the increasing of pH value, hexagonal phase becomes weak and cubic phase becomes strong gradually and when the pH value reaches to 10, pure cubic phase $NaYF_4$ IOPCs are formed. In addition to pH value, the reaction time is another important parameter, which has great impact on the location of PBG and the details can be seen in Fig. S1.

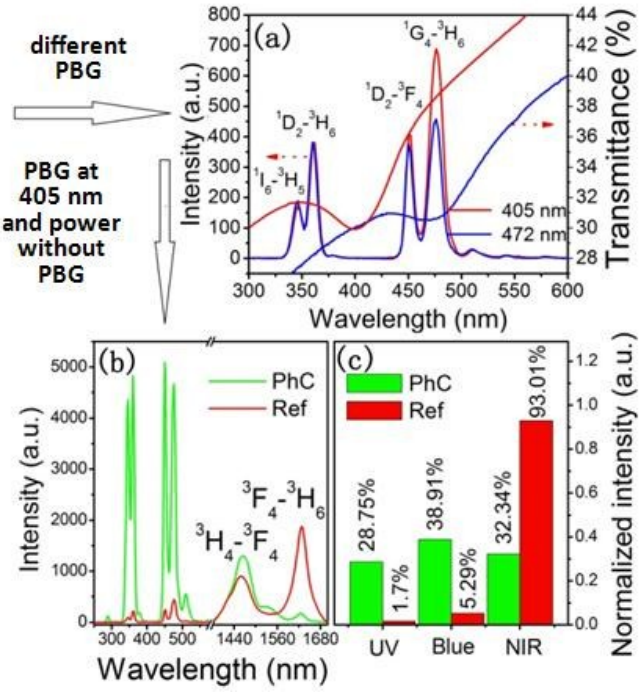

Fig. 3(a) The steady-state spectra of $NaYF_4$: Yb^{3+}, Tm^{3+} IOPCs with PBGs at 405 nm and 472 nm (980 nm, 0.33W/mm^2). (b) The steady-state spectra of $NaYF_4$: Yb^{3+}, Tm^{3+} IOPCs with PBGs at 405 nm and the corresponding powder (980 nm, 0.63W/mm^2). (c) The proportion of different colors in total luminescence intensity (980 nm, 0.63W/mm^2).

Fig.3(a) shows the steady-state emission spectra(980 nm, 0.33W/mm^2)and the transmittance spectra at normal (θ=0^o) of $NaYF_4$: 20%Yb^{3+}, 0.5%Tm^{3+} IOPCs with PBGs at 405 nm (PhC1) and 472 nm (PhC2). Note that PHC1 and PHC2 were obtained by controlling the size of PMMA spheres, and the hydrothermal reaction times were both fixed at 3h. It can be seen that while the PBG overlaps with the $^1G_4$-$^3H_6$ and $^1D_2$-$^3H_6$ transition of Tm^{3+} (PhC2), a significant inhibition of luminescent intensity can be observed in contrast to PhC1. This is due to the reduction in the number of optical modes available for photon propagation at frequencies within the PBGs. The inhibition of light emission is a universal phenomenon for luminescent species embedded in PhCs. Noted that the luminescence dynamic processes are not modified by PBG effect (see Fig. S2) and this phenomenon is similar to our previous works.[9]

Fig.3(b) shows the steady-state emission spectra of $NaYF_4$: 20%Yb^{3+}, 0.5%Tm^{3+} IOPC (PBG ~ 405nm) and the corresponding grinded powders of $NaYF_4$: 20%Yb^{3+}, 0.5%Tm^{3+} IOPC (Ref) and 3(c) shows the proportion of different transitions in total luminescent intensity (980 nm, 0.63W/mm^2).For Ref sample, the down-conversion NIR luminescent intensity is absolute predominant (93.01%), while that is only 32.34% in the PhC sample. Surprisingly, the percentage of visible UCL improves from 5.29 % of the REF to 38.91 % of the IOPC, while UV light improves from 1.7% to 28.75%. In one word, the UCL processes, especially the high-order processes in IOPC sample have been greatly improved in contrast to the Ref sample.

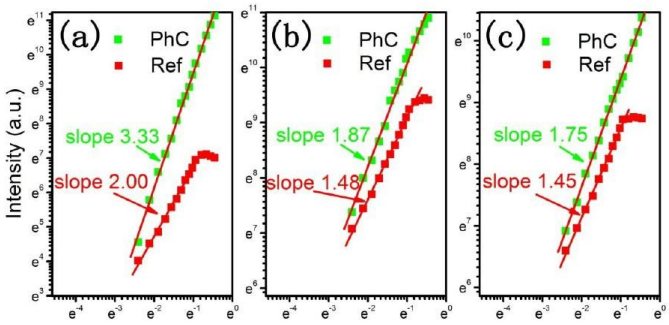

Fig.4 The power dependent UCL intensity of different transitions in $NaYF_4$: Yb^{3+}, Er^3+ IOPCs and REF samples.

In order to reveal the mechanism of UCL, the double-logarithmic plots of the UCL intensity of different transitions were as a function of excitation power density under 980-nm excitation, as shown in Figure 4. It can be seen that the slopes n of $^4H_{9/2}$-$^4I_{15/2,}$ $^2H_{11/2}$/$^4H_{13/2}$-$^4I_{15/2+}$, and $^4F_{9/2}$-$^4I_{15/2}$ in $NaYF_4$: Yb^{3+}, Er^{3+} IOPCs were larger than that in REF samples. In addition, with the increasing of the excitation power density, the slopes of REF sample gradually decreased, which was mainly attributed to the improved saturation effect and local thermal effect induced by laser exposure, but the slopes of $NaYF_4$: Yb^{3+}, Er^{3+} IOPCs changed a little. This is the reason that the IOPC structure could suppress the local thermal effect.

Based on virtual cavity model,[10] the radiative transition rate W_R can be approximatively expressed as:

$$W_R \approx f(\mathrm{ED}) \frac{\left[\frac{1}{3}(n_{eff}{}^2+2)\right]^2 n_{eff}}{\lambda_0{}^2}, \quad (1)$$

Where *f(ED)* is electric dipole strength, λ_0 is the wave length in vacuum, n_{eff} is effective refractive index. Through calculation, n_{eff} in IOPC (n_{eff}=1.25) is less than n_{eff} in Ref (n_{eff}=1.72), so W_R in IOPC should be less than that in the Ref based on equation (1). Note that under the excitation of the 980 nm light with the same power density, the IOPC sample has a lower temperature increase, (see Fig S3). This also indicates that the IOPC structure can suppress the local thermal effect induced by laser irradiation, which is attributed to its better thermal diffusion property due to the empty cavity structure. So it can be concluded that the nonradiative relaxation rate W_{NR} in IOPC should be also less than that in Ref because of the increased phonon density, which depends strongly on temperature. The lower W_R(PhC) and W_{NR}(PhC) leads to longer intermediate state lifetime, make electrons transit into higher energy level more easily.

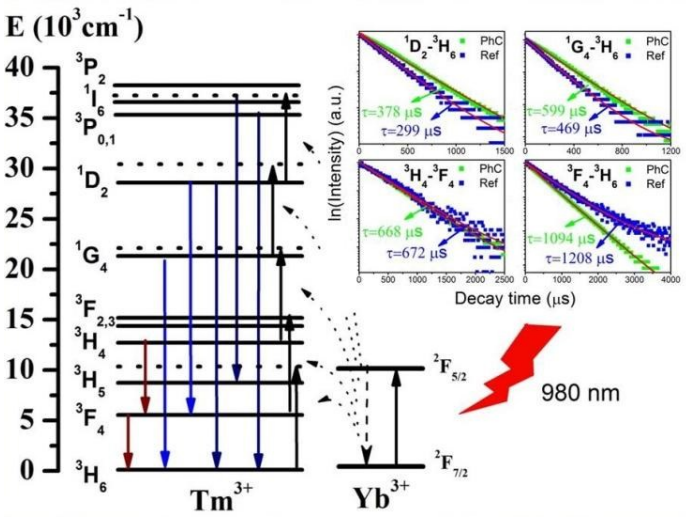

Fig. 5 The energy-level diagram of Yb^{3+}, Tm^{3+} under 980-nm excitation. Inset: the lifetime of different energy levels of Tm^{3+}.

UCL dynamics are a powerful method to understand the microscopic processes. In order to better understand the UCL property of $NaYF_4$ IOPCs, the luminescent dynamic processes of $^1D_2$-$^3H_6$, $^1G_4$-$^3H_6$, $^3H_4$-$^3F_6$ and $^3F_4$-$^3H_6$were investigated and shown in the upper right of Fig. 5. As shown, the lifetimes of $^1D_2$-$^3H_6$ and $^1G_4$-$^3H_6$ in IOPC sample are prolonged 25% and 27% compared to Ref sample, respectively. Instead, the lifetime of $^3H_4$-$^3F_4$ is similar but that of $^3F_4$-$^3H_4$ becomes smaller. As is well known, the lifetime of one luminescent state is reciprocal to radiative transition rates plus nonradiative relaxation rates. Normally, the nonradiative processes only occur from the excited energy level to the nearest down energy level. However, in the UCL system, the electron in the excited energy level can absorb a photon and transit into a higher energy level, which is also a nonradiative process. So the lifetime τ can be expressed as:

$$\tau = \frac{1}{W_R + W_{NR} + W_{UP}}, \quad (2)$$

Where W_R is radiative transition rate, W_{NR} is nonradiative relaxation rate and W_{UP} is up-conversion transition rate. W_R(PhC) becomes small duo to the modulations of effective refractive index and W_{NR}(PhC) also turns small because the local temperature is lower in contrast to powder samples (this can be deduced by the ratio of green light intensity of Er^{3+} ions and seen in Fig. S3). Note that, the inhibition of local temperature also restrain the nonradiative processes of Yb^{3+} ions, leading to the energy transition from Yb^{3+} to Tm^{3+} becomes much easier.[11] As well known, lifetime plays an important role in UC processes and the long lifetime is conduce to UCL. Base on equation (2), for $^3F_4$ energy level, W_{UP}(PhC) changes significantly and plays a dominant role (lifetime is long enough), so the lifetime of $^3F_4$-$^3H_4$ becomes smaller; and for $^1D_2$ and $^1G_4$, W_{UP}(PhC) changes weakly (lifetime is short), so the lifetime of $^1D_4$-$^3H_6$ and $^1G_4$-$^3H_6$ are prolonged.

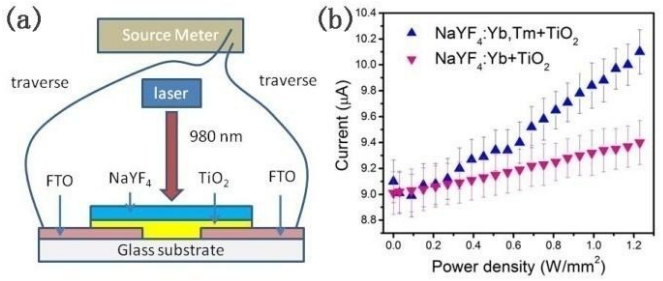

Fig. 6(a) The schematic diagram of $NaYF_4/TiO_2$ NIR photoelectric response system. (b) The current of $NaYF_4/TiO_2$composite structure with different power density (+5V voltage is applied).

The energy gap of anatase TiO_2 structure is about 3.2 eV, a UC photon with enough energy (UV UCL of $^1D_2$-$^3H_6$ and $^1I_6$-$^3I_5$) can be absorbed by TiO_2 and generates a photoelectron. Fig. 6(a) shows the schematic diagram of $NaYF_4/TiO_2$ NIR photoelectric response system. Note that in the system, a 2 mm gap in the middle of FTO was etched by hydrochloric acid, then a polycrystalline anatase TiO_2 film was grown by magnetron sputtering and then the $NaYF_4$ IOPC was adhered to the TiO_2 film. The photocurrent was measured by a Source Meter with a voltage of 5Vunder the irradiation of a 980 nm continuous laser. Each test point was measured by 40 times. The average values and the error bars were shown in Fig. 6(b). A ~9μA dark current was measured without irradiation and the current became stronger when the power density was up to 0.3 W/mm^2, which was corresponding to UCL threshold of $NaYF_4$: Yb, Tm IOPCs. The current finally enhanced 12% when the power density reached to 1.25 W/mm^2. In order to exclude the influence of local thermal effect, the situation without Tm^{3+} doping was considered and the current was enhanced only 3.8% at 1.25 W/mm^2, implying that the NIR to UV UCL played a dominant role for the improvement of photocurrent with excitation power in $NaYF_4$: Yb, Tm IOPC/TiO_2 composites. Actually, we used the corresponding grinded powder of IOPC adhered on the TiO_2 film with the same quantity to measure the photocurrent. But the photocurrent was too weak to detect expect the dark current, showing that the netware structure of IOPCs is helpful of electron transport.

Conclusions

In summary, $NaYF_4$ IOPCs were successfully prepared through a novel solvent-thermal Y_2O_3 template method and the phase of $NaYF_4$ and the PBG of IOPCs could be adjusted by pH value, reaction time and the template. It is significant to observe that $NaYF_4$:Tm^{3+}/Er^{3+}, Yb^{3+} IOPCs showed an extraordinarily improved UCL ratio in contrast to the REF. And more, the NIR photoelectric response was observed in $NaYF_4$: Yb, Tm IOPCs/TiO_2 system, which shows potential applications in NIR photocatalyses and degradations.

Acknowledgements

This work was supported by the Major State Basic Research Development Program of China (973 Program)(No. 2014CB643506), the National Natural Science Foundation of China(No.81301289,11374127,11304118,61204015, 81201738,61177042, and 11174111), Program for Chang Jiang Scholars and Innovative Research Team in University (No. IRT13018), Youth Research Fund Project of Jilin Province Science and Technology Development Plan (No. 20130522032JH, 20130522039JH).

References

1 (a) F. Zhang, Y. Wan, T. Ying, F.Q. Zhang, Y.F. Shi, S.H. Xie, Y.G. Li, L. Xu, B. Tu, and D.Y. Zhao, *Angew. Chem., Int. Ed.*, 2007, **46**, 7976; (b) F. Wang, and X.G. Liu, *Chem. Soc. Rev.*, 2009, **38**, 976; (c) R.R. Deng, X.J. Xie, M. Vendrell, Y.T. Chang, and X.G. Liu, *J. Am. Chem. Soc,* 2011, 133, 20168; (d)Mai H.X, Zhang Y.W, Si R, Yan Z.G, and C.H. Yan, *J. Am. Chem. Soc.,* 2006, **128**, 6426.
2 Y.S. Liu, S.Y. Zhou, D.T. Tu, Z. Chen, M.D. Huang, H.M. Zhu, E. Ma, and X.Y .Chen, *J. Am. Chem. Soc.*, 2012, **134**, 15083.
3 (a) P. Huang, W. Zheng, S.Y. Zhou, D.T. Tu, Z. Chen, H.M. Zhu, R.F. Li, E. Ma, M.D. Huang, and X.Y. Chen, *Angew. Chem. Int. Ed.,* 2014, **53**, 1252; (b) Y.S. Lin, Y. Hung, H.Y. Lin, Y. H. Tseng, Y. F. Chen, and C. Y. Mou, *Adv. Mater.,* 2007, **19**, 577; (c) L. L. Tao, B. Zhou, W. Jin, Y. Chai, C. Y. Tang, and Y. H. Tsang, *Opt. Lett.,*2014, **39**, 6265.
4 E. Yablonovitch, *Phys. Rev. Lett,* 1987, **58**, 2059.
5 S. John, *Phys. Rev. Lett,* 1987, **58**, 2486.
6 (a) S. Y. Lin, E. Chow, V. Hietala, P. R. Villeneuve, and J. D. Joannopoulos, *Science,* 1998, **282**, 274; (b) P. W. Zhou, D. L. Zhou, L. Tao, Y. S. Zhu, W. Xu, S. Xu, S. B. Cui, L. Xu, and H. W. Song, *Light Sci Appl,* 2014, **3**, e209; (c) S. G. Romanov, A. V. Fokin, and R. M. De La Rue, *Appl. Phys. Lett.*,1999, **74**, 1821.
7 (a) D. Wang, A. L. Rogach, and F. Caruso, *Chem. Mater.*, 2003, **15**, 2724; (b) I. S. Nikolaev, P. Lodahl, and W. L. Vos, *J. Phys. Chem. C,* 2008,**112**, 7250.
8 (a) Z. X. Li, L. L. Li, H. P. Zhou, Q. Yuan, C. Chen, L. D. Sun, and C. H. Yan, *Chem. Commum.*,2009, **43**, 6616; (b) F. Zhang, Y. H. Deng, Y. F. Shi, R. Y. Zhang, and D. Y. Zhao, *J. Mater. Chem.*, 2010, **20**, 3895.
9 L. Tao, W. Xu, Y. S. Zhu, L. Xu, Y. X. Liu, S. Xu, P. W. Zhou, and H. W. Song, *J. Mater. Chem. C*, 2014, **2**, 4186.
10 S.B. Cui, Y.S. Zhu, W. Xu, P.W. Zhou, L. Xia, X. Chen, H.W. Song, and W .Han, *Dalton Trans*., 2014, **43**, 13293.
11 (a) Y.S. Zhu, W. Xu, H.Z. Zhang, S. Xu, Y.F. Wang, Q.L. Dai, , B. Dong, L. Xu, and H.W. Song, *Opt. Lett.,* 2012, **20**,29673; (b) W. Yu, W. Xu, H.W. Song, and S. Zhang, *Dalton Trans.*, 2014, **43**, 6139.

Table of contents

A novel solvent-thermal Y_2O_3 template method was explored to synthesis $NaYF_4:Yb^{3+},Tm^{3+}$ IOPCs, which shows highly improved UCL properties.

Yudan Yang, [ba] Pingwei Zhou, [a] Wen Xu,[a] Sai Xu, [a] Yandong Jiang, [a] Xu Chen[a] and Hongwei Song*[a]

$NaYF_4:Yb^{3+},Tm^{3+}$Inverse Opal Photonic Crystals and $NaYF_4:Yb^{3+},Tm^{3+}/TiO_2$composites: Synthesis, Highly Improved Upconversion Properties and NIR Photoelectric Response